FOOD AND BIOPRODUCTS PROCESSING xxx (2016) xxx–xxx

Contents lists available at ScienceDirect

Food and Bioproducts Processing

journal homepage: www.elsevier.com/locate/fbp

Computer simulation model development and validation of radio frequency heating for bulk chestnuts based on single particle approach

Lixia Hou[a], *Zhi Huang*[a], *Xiaoxi Kou*[a], *Shaojin Wang*[a,b,*]

[a] *College of Mechanical and Electronic Engineering, Northwest A&F University, Yangling, Shaanxi 712100, China*
[b] *Department of Biological Systems Engineering, Washington State University, 213 L.J. Smith Hall, Pullman, WA 99164-6120, USA*

ARTICLE INFO

Article history:
Received 19 December 2015
Received in revised form 22 June 2016
Accepted 18 August 2016
Available online xxx

Keywords:
Chestnut
Computer simulation
Heating uniformity
RF heating
Single particle

ABSTRACT

A computer simulation model was developed using finite element-based commercial software, COMSOL, to simulate temperature distributions of single particle chestnuts packed in a rectangular plastic container and treated in a 6 kW, 27.12 MHz radio frequency (RF) system. The developed model was validated by temperature distributions of three horizontal layers and temperature profiles at three representative positions in the container without mixing. Both simulated and experimental results showed similar heating patterns in RF treated chestnuts under same conditions, in which corners and edges were overheated and highest temperatures were located in sample contact points of top and middle layers at four corners in the container. A heating uniformity index (HUI) was used to evaluate effects of processing conditions on RF heating uniformity. The simulated and experimental results showed that the HUI was reduced when three layers chestnuts were separated with two plastic sheets. The better heating uniformity in chestnuts was obtained when they were treated with a single layer, or under mixing conditions. The developed model can help to explore the RF heating patterns on a single particle chestnut and RF heating uniformity in chestnuts of the container, and provide valuable methods to improve the RF heating uniformity for future industrial applications.

1. Introduction

Chestnut (*Castanea mollissima*) is a widely consuming nut around the world due to its special flavor and taste. Since postharvest chestnuts contain high moisture content, rich carbohydrate, and low fat (Chenlo et al., 2009; Vasconcelos et al., 2010), infestations with pests and diseases are major issues on chestnuts during long term storage (Antonio et al., 2011). It is estimated that annual losses of chestnuts due to pests are about 35–50% of total production during storage in China, resulting in high economic losses (Gao et al., 2011). Chemical fumigation with methyl bromide has been widely used to disinfest agricultural products, including chestnuts. However, this chemical fumigation is harmful to not only human's health but also environment due to depleting ozone layer. Therefore, various alternatives for disinfestations, such as ozone, modified atmospheres, low pressure and low temperature, irradiation, etc. have been studied (Carocho et al., 2012; Jiao et al., 2013; Pan et al., 2012). Although there are a large number of suggested potential chemical and non-chemical alternatives for disinfestations, each has limitations in terms of efficiency, cost, penetration, or residues that prevent it from becoming a direct replacement for pesticides (Hansen et al., 1992). Recently, radio frequency (RF) energy is proposed as an effective and environmental-friendly heating method to control insects in nuts and grains, including chestnuts, with acceptable product quality (Gao et al., 2010; Hou et al., 2015a; Jiao et al., 2012; Wang et al., 2007b).

* *Corresponding author at*: College of Mechanical and Electronic Engineering, Northwest A&F University, Yangling, Shaanxi 712100, China. Fax: +86 29 87091737.
E-mail address: shaojinwang@nwsuaf.edu.cn (S. Wang).

http://dx.doi.org/10.1016/j.fbp.2016.08.008
0960-3085/

Nomenclature

A	Surface area (m^2)
C_p	Heat capacity ($J\,kg^{-1}\,{}^\circ C^{-1}$)
E	Electric field intensity ($V\,m^{-1}$)
f	Frequency (Hz)
h	Heat transfer coefficient at the same surface ($W\,m^{-2}\,{}^\circ C^{-1}$)
HUI	Heating uniformity index (dimensionless)
k	Thermal conductivity ($W\,m^{-1}\,{}^\circ C^{-1}$)
Q	Power density generated by electric field ($W\,m^{-3}$)
t	Time (s)
T	Sample temperature (°C)
T_{av}	Average temperature (°C)
$T_{initial}$	Initial average temperature of chestnuts (°C)
ΔT	Temperature difference (°C)
Δt	Total time taken during each mixing process (s)
$\partial T/\partial t$	Increase rate of temperature ($^\circ C\,s^{-1}$)
V	Electric potential (V)
V_{vol}	Volume (m^3)
ε	Permittivity ($F\,m^{-1}$)
ε_0	Free space permittivity ($F\,m^{-1}$)
ε'	dielectric constant (dimensionless)
ε''	Dielectric loss factor (dimensionless)
∇	Gradient operator
ρ	Density ($kg\,m^{-3}$)

Heating non-uniformity is one of the major obstacles for RF technology to be commercially applicable, especially in samples with high moisture contents and large sizes, such as chestnuts. It is reported that several interacting factors (e.g., electrode gap, electrode shape, packing geometries, position of treated sample, and surrounding media) influence heating uniformity during RF treatments (Huang et al., 2015c; Jiao et al., 2015; Tiwari et al., 2011a,b). However, experimental methods to adjust these parameters are time consuming, costly, and often provide limited information. On the contrary, computer simulation can be served as an effective tool for rapid, cheap, and flexible analysis, and provide an insight into the dielectric heating mechanism in agricultural products (Hossan et al., 2010; Romano and Marra, 2008; Tiwari et al., 2011a). To help understand the complex RF dielectric heating process and analyze RF heating uniformity, simulation has previously been used in various products, such as dry soybeans (Huang et al., 2015c), eggs (Dev et al., 2012), fruit (Birla et al., 2008),meat batters (Romano and Marra, 2008), peanut butter (Jiao et al., 2014), raisins (Alfaifi et al., 2014), wheat (Chen et al., 2015), and wheat flour (Tiwari et al., 2011b).

Agricultural products, such as fruits and nuts, in bulk may contain a certain amount of air among the product particles. On the one hand, air reduces flow of heat throughout the material during RF treatments. On the other hand, dielectric properties and thermal conductivity of air are totally different from those of fruits and nuts. Therefore, mixing equations are used to estimate effective dielectric properties and thermal conductivity of the air–particle mixture made up of air (voids) and particles of the solid (Nelson, 1991). Alfaifi et al. (2014) used mixing equations to calculate dielectric and thermal conductivity of raisins in container, and determined heating uniformity of the raisin in the container as a whole sample during RF heating. They found that heating uniformity in raisins was mostly affected by density of the raisin followed by the top electrode voltage, the dielectric properties, the thermal conductivity, and the heat transfer coefficient. Similar mixing equations have been applied to simulate RF heating on dry soybeans (Huang et al., 2015c), meat batters (Uyar et al., 2016), wheat (Chen et al., 2015), and wheat flour (Tiwari et al., 2011b). However, container's shape and size are totally different from those of samples, resulting in poor RF heating uniformity (Tiwari et al., 2011a). Therefore, it is necessary to determine the temperature distribution of RF treated bulk nuts and a single nut, which has not been reported so far using the finite element simulation.

The objectives of this research were to (1) develop a computer simulation model for bulk chestnuts based on a single particle approach when subjected to a 6 kW, 27.12 MHz RF system using commercial finite element software COMSOL, (2) validate the computer simulation model by comparing with the experimental temperature profiles of chestnuts after 5.4 min RF heating, (3) apply the validated model to predict the behavior of RF heating non-uniformity in bulk chestnuts and the single particle chestnut, and (4) explore effective methods to improve the RF heating uniformity in chestnuts.

2. Materials and methods

2.1. Sample preparation

Chinese chestnuts (*C. mollissima*) were purchased from a local wholesale market in Yangling, Shaanxi Province, China. The average initial moisture content and individual weight of tested chestnuts were 51.27 ± 1.19% on wet basis (w.b.) and 11.71 ± 0.91 g, respectively. The chestnuts were stored with mesh bags in a refrigerator (BD/BC-297KMQ, Midea Refrigeration Division, Hefei, China) at 4 ± 1 °C, taken out from the refrigerator 12 h before the experiment, and kept at ambient room temperature (20 ± 1 °C) for equilibrium.

2.2. Simulation model development

2.2.1. Physical model

A 6 kW, 27.12 MHz parallel electrodes, pilot scale free-running oscillator RF unit (SO6B, Strayfield International Limited, Wokingham, UK) was used in this research, with an area of 83 × 40 cm^2 for top plate electrode and a larger bottom plate electrode (Fig. 1). In the RF cavity (2.98 m long, 1.09 m wide and 0.74 m high), about 2.5 kg chestnuts were filled into a polypropylene plastic container (24 × 18 × 6 cm^3), and placed on the center of the bottom electrode, for RF treatments. The electrode gap was changed by adjusting position of the top electrode to achieve the required the RF power and heating rate.

It was considered that there are three layers chestnuts in the container with 72 chestnuts in each layer. Individual weight and density of tested chestnuts were 11.71 ± 0.91 g and 1.22 ± 0.03 g/cm^3, respectively. Chestnut was simplified as an ellipsoid shape in the simulation model. The sizes of *a*, *b*, and *c* in semi-principal axes were selected as 1.5 cm, 1.5 cm, and 1.0 cm, respectively, to achieve a small volume difference between the real chestnut and the simplified ellipsoid model.

2.2.2. Governing equations

The Maxwell's equations can be used to solve the electric field intensity in the electromagnetic field. Since the RF wavelength (11 m) in the 27.12 MHz RF unit is often much longer than the RF cavity size, the Maxwell's equation can be simplified to the Laplace equation by neglecting the effect of magnetic fields. The Laplace equation is described by a quasi-static assumption (Birla et al., 2008): Q4

$$-\nabla \cdot ((\sigma + j2\pi f \varepsilon_0 \varepsilon')\nabla V) = 0 \quad (1)$$

where σ delegates electrical conductivity of the treated sample or air ($S\,m^{-1}$) and ε' represents also dielectric constant of treated sample or air, depending on which domain the equation is solved. $j = \sqrt{-1}$, f is the frequency (Hz), ε_0 is the permittivity of free space (8.86 × 10^{-12} $F\,m^{-1}$) and V delegates the

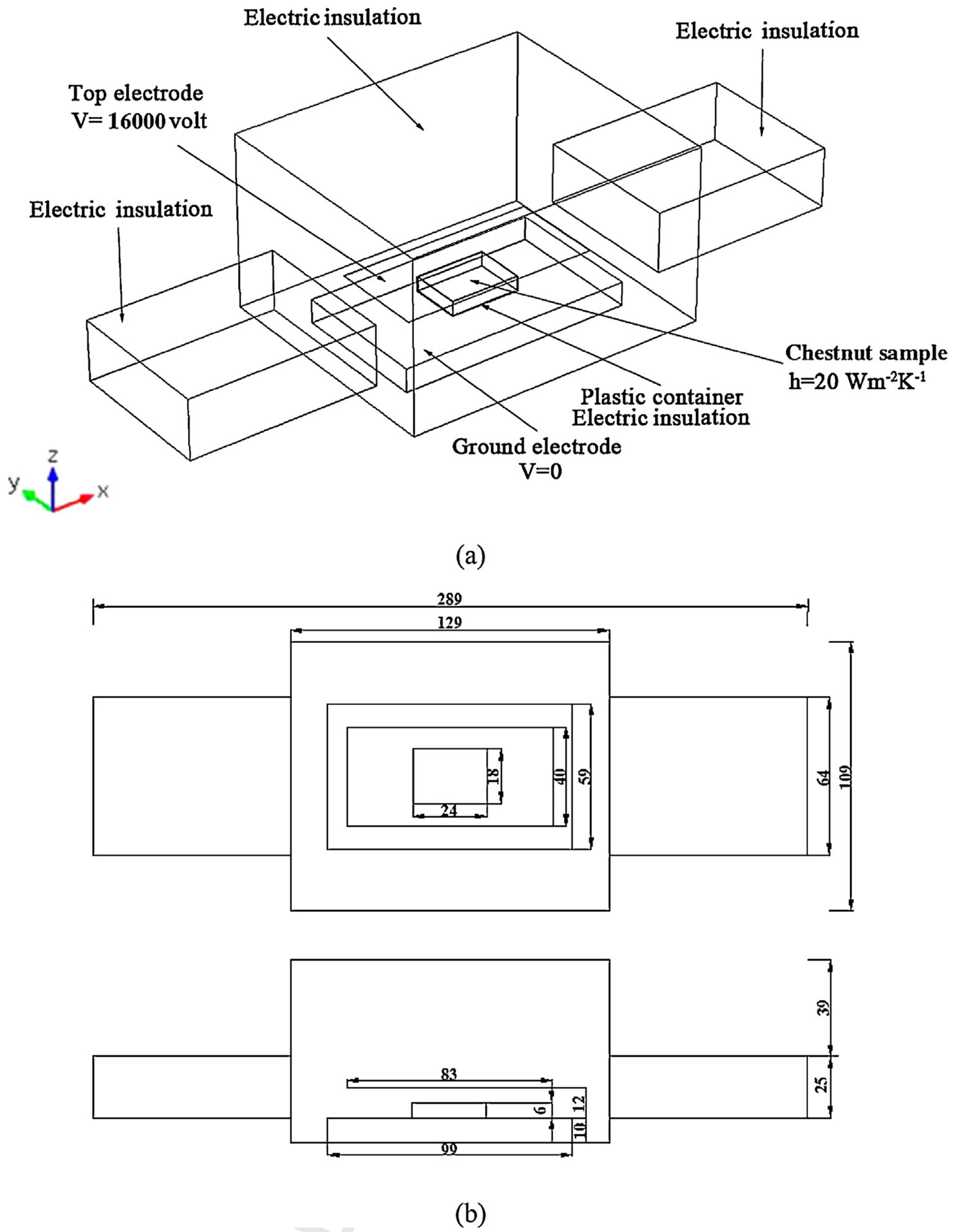

Fig. 1 – 3-D scheme (a) and dimensions (b) of the 6 kW 27.12 MHz RF system and chestnuts used in simulations (all dimensions are in cm).

voltage (V) between the two electrodes related to the electric field ($E = -\nabla V$).

When a dielectric material is placed between two plate RF electrodes, the RF power (Q, W m^{-3}) in the material, conversed to thermal energy, can be described as (Choi, 1991):

$$Q = 2\pi f \varepsilon_0 \varepsilon'' |\vec{E}|^2 \quad (2)$$

where the electric field intensity is $\vec{E} = -\nabla V$, ε'' is the loss factor of the treated sample.

The heat conduction equation was just solved within the treated sample, convection at the sample's surface and heat generation in the chestnuts due to RF energy. The heat transfer inside the treated sample is described by Fourier's equation (Uyar et al., 2015):

$$\rho C_p \frac{\partial T}{\partial t} = \nabla \cdot (k \nabla T) + Q \quad (3)$$

where $\partial T/\partial t$ is heating rate in treated samples (°C s^{-1}), k is thermal conductivity (W m^{-1} K^{-1}), ρ and C_p are density (kg m^{-3}) and specific heat (J kg^{-1} K^{-1}) of treated samples, respectively.

2.2.3. *Initial and boundary conditions*

The geometrical, thermal and electrical boundary conditions of the RF unit used in the computer simulation model are illustrated in Fig. 1. The initial temperature was set at 20 °C. Except for that the top surface of chestnuts was uncovered and exposed to the ambient air, the side walls and bottom of the chestnuts were surrounded by the rectangular plastic container (Fig. 1a). The top exposed surface of the sample was assigned with convective heat transfer (h = 20 W m^{-2} K^{-1}) for free convection of ambient air (Wang et al., 2001). Electrode gap between the top and bottom plates was set as 12 cm to acquire the suitable heating rate of treated chestnuts (Hou et al., 2014). The top electrode was deemed as the electromagnetic source since it inputted high frequency electromagnetic energy from the generator to the RF cavity and the bottom electrode was considered as ground (V = 0 V). It was difficult to measure the actual top electrode voltage during operating without disturbing the heating operation (Marshall and Metaxas, 1998), therefore, preliminary simulations with the same conditions were run by considering different values of top electrode voltage. Based on the comparison between preliminarily simulated and experimental sample temperature distributions, the top electrode voltage was considered as 16,000 V for the final simulation. The same approach has been used to evaluate top electrode voltage of similar RF units (Birla et al., 2008; Chen et al., 2015; Huang et al., 2015a; Marshall and Metaxas, 1998; Tiwari et al., 2011b). All the metal shielding parts except for the top electrode were grounded, and considered as electrical insulation ($\nabla E = 0$).

2.2.4. *Simulation procedure*

A finite element analysis software, COMSOL Multiphysics 4.3a (COMSOL Multiphysics, CnTech Co., Ltd., Wuhan, China), was used to solve the coupled electromagnetic and heat transfer equations (Joule heating model). The software was run on a ThinkPad PC with an Intel Core i5-4210U, 2.40 GHz Quad Core Processor and 8 GB RAM with a Windows 7 64-bit operating system. COMSOL provides normal, fine, finer, extra fine, and extremely fine meshes. According to accuracy and resource consumption, a finer mesh was used to establish the final mesh system, which consisted of 109,364 domain elements (tetrahedral) used in subsequent simulation runs. Each computation case took about 30 min to complete.

2.2.5. *Model parameters*

Information of dielectric, physical, and thermal properties of the treated chestnuts and surrounding medium is essential in modeling the RF heating process. Since thermal properties of food depend mostly on compositions, heat capacity and thermal conductivity can be calculated (Sahin and Sumnu, 2006). According to the literatures (Hou et al., 2014; Korel and Balaban, 2006), moisture content, carbohydrate, protein, fat, and ash of chestnuts were 51.27%, 38.82%, 2.03%, 5.94%, and 2.46%, respectively. The thermal conductivity (k) and specific heat (C_p) of chestnuts were calculated by the following equations (Sahin and Sumnu, 2006):

$$k = 0.5127 \times k_{water} + 0.3882 \times k_{CHO} + 0.0203 \times k_{protein} + 0.0594 \times k_{fat} + 0.0246 \times k_{ash} = 0.39343 + 1.336967 \times 10^{-3} T - 5.25552 \times 10^{-6} T^2 \quad (4)$$

$$C_p = 0.5127 \times C_{p\,water} + 0.3882 \times C_{p\,CHO} + 0.0203 \times C_{p\,protein} + 0.0594 \times C_{p\,fat} + 0.0246 \times C_{p\,ash} = 2927.89 + 0.87156 \times T + 0.09781 \times 10^{-3} T^2 \quad (5)$$

where T is the sample temperature (°C).

Table 1 lists heat capacity, density, thermal conductivity, and dielectric properties of chestnuts, polypropylene, aluminum and air used in the computer model. The density was assumed to be temperature independent, whereas the heat capacity, thermal conductivity, and dielectric properties of chestnuts were assumed to be temperature dependent over the range of treatment temperatures (20–60 °C).

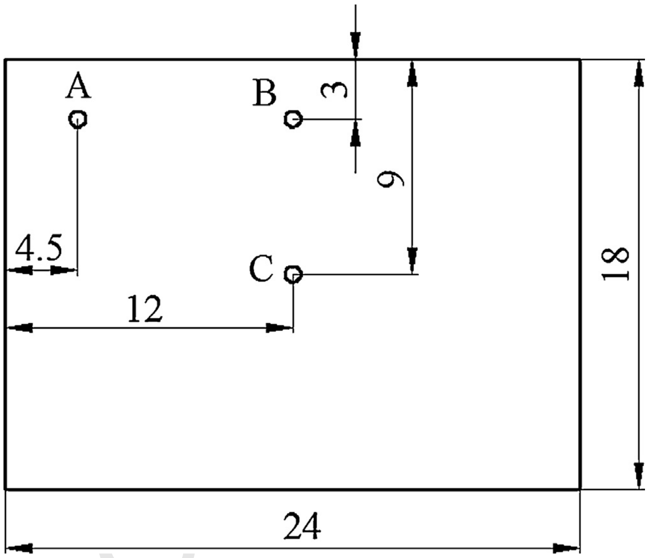

Fig. 2 – Three positions (A–C) used to measure the temperature-time history of chestnuts in the middle layer during RF treatments (all dimensions are in cm).

2.2.6. *RF heating uniformity index of the sample*

Heating uniformity index (λ) was successfully used for evaluating RF heating uniformity in coffee bean (Pan et al., 2012), lentil (Jiao et al., 2012), almond (Gao et al., 2010), chestnut (Hou et al., 2014), and walnut (Wang et al., 2007a). It is defined as (Alfaifi et al., 2014):

$$HUI = \frac{\frac{1}{V_{vol}} \int V_{vol} sqrt((T - T_{av})^2) dV_{vol}}{T_{av} - T_{initial}} \quad (6)$$

where T and T_{av} are local and average temperatures (°C) inside the chestnuts over the volume (V_{vol}, m^3), $T_{initial}$ is initial average temperature of chestnuts (°C) before RF treatments. In a RF treatment, a smaller HUI indicates better heating uniformity. Ideal value of HUI is zero, which means all the chestnuts gain the same temperature.

2.3. *Model validation*

2.3.1. *Experiment without mixing*

To validate the developed computer simulation model, the plastic container filled with 2.5 kg of chestnuts was put on the bottom electrode in the center of RF cavity and heated by the RF unit. Target average temperature for complete kill of insect pests in chestnuts with acceptable quality was estimated to be 50 °C for 3 min, based on the thermal-death kinetics of yellow peach moth (Hou et al., 2015a; Moreira et al., 2011, 2013). Therefore, the target temperature of treated chestnuts was set as 50 °C. A fiber optic sensor (HQ-FTS-D120, Xi'an HeQi Opo-Electronic Technology Co., LTD, Shaanxi, China) was inserted into chestnuts at a predetermined position to obtain temperature-time history (Fig. 2). The heating time needed for the cold spot from ambient temperature (20 °C) to 50 °C was recorded. When the cold spot reached 50 °C, the sample was taken out immediately to take thermal images. The obtained temperature profiles were further used to validate the computer simulation model. A thermal digital infrared camera (DM63-S, DaLi Science and Technology Co., LTD, Zhejiang, China) with an accuracy of ±2 °C was used for mapping the surface temperatures of chestnuts in top, middle, and bottom layers after the treated chestnuts were taken out from the

Please cite this article in press as: Hou, L., et al., Computer simulation model development and validation of radio frequency heating for bulk chestnuts based on single particle approach. Food Bioprod Process (2016), http://dx.doi.org/10.1016/j.fbp.2016.08.008

Q8 **Table 1 – Electrical and thermo-physical properties of bulk materials used in computer simulation.**

Material properties	Chestnut	Aluminum[a]	Air[a]	Polypropylene[a]
Heat capacity C_p (J kg^{-1} K^{-1})	$0.8794 \times T + 2927.75$	900	1200	1800
Density ρ (kg m^{-3})	1221.74	2700	1.2	900
Thermal conductivity k (W m^{-1} K^{-1})	$0.00092 \times T + 0.40079$	160	0.025	0.2
Dielectric constant (ε')	$0.014 \times T \times T - 0.515 \times T + 35.46$[c]	1	1	2.0[b]
Loss factor (ε'')	$0.058 \times T \times T - 1.825 \times T + 58.46$[c]	0	0	0.0023[b]

T = temperature (°C).
[a] COMSOL material library, V4.3a (2012).
[b] von Hippel (1995).
[c] Guo et al. (2011).

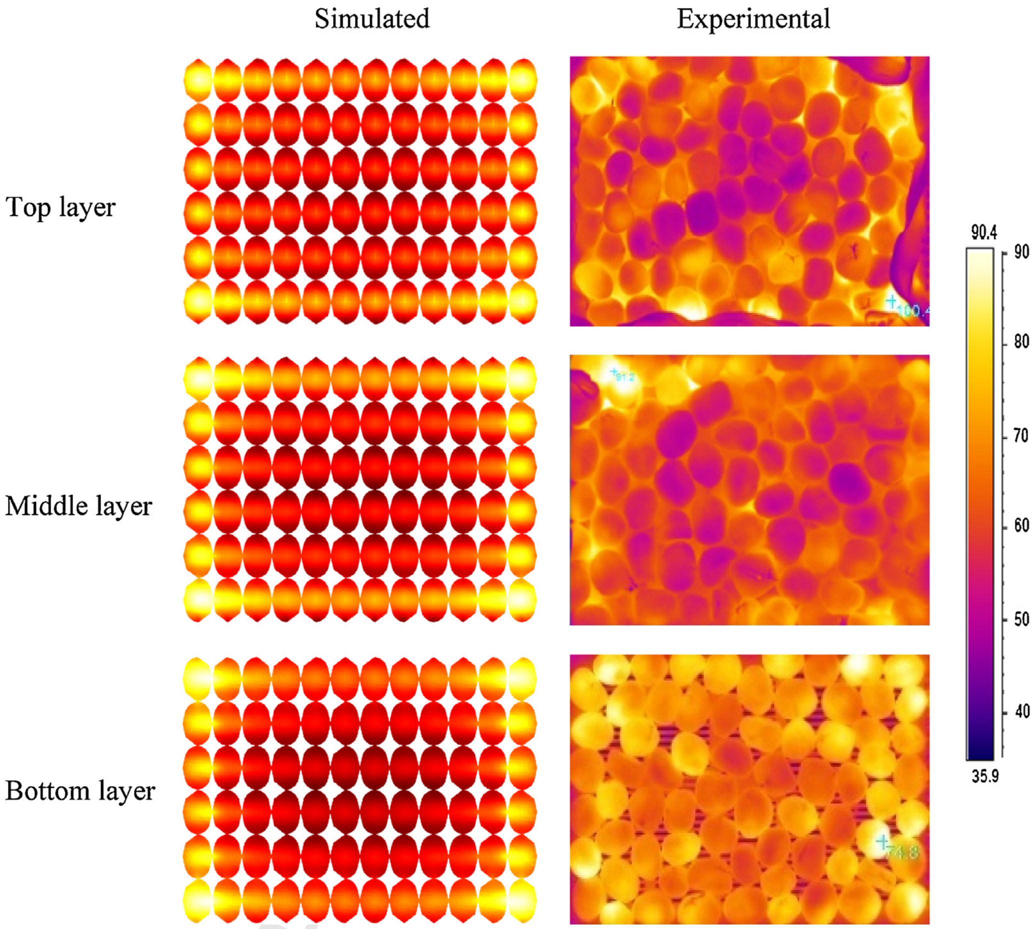

Fig. 3 – Comparison of simulated and experimental temperature distributions for top, middle, and bottom layers of chestnuts placed in a polypropylene container (24 × 18 × 6 cm^3) on the bottom electrode after RF heating.

RF cavity. The thermal digital infrared camera was first calibrated against a thin thermocouple thermometer (HH-25TC, Type-T, OMEGA Engineering Inc., Stamford, Connecticut, USA) with an accuracy of ±0.5 °C and 0.9 s response time. The whole temperature measurement procedure was completed within 20 s. The experiments were replicated three times.

2.3.2. *Mixing experiments*

The same sample was used for mixing experiments with an electrode gap of 120 mm during the whole 5.4 min RF heating. The experiments were carried out at intervals of 1.8 min for two mixing treatments during entire treatment time. Mixing was conducted manually outside the RF cavity in a larger container (35.5 × 27.5 × 10.5 cm^3) for 25 s, and then the samples were returned to the container and put back into the RF system for further heating under the same conditions. After the two mixing processes were completed, samples were placed back into the RF cavity for the remainder of the heating time. Each whole mixing process took about 60 s. Before and immediately after RF treatments, surface temperatures of the top layer chestnuts in the container were measured with the same infrared camera described above. Each measurement took about 3 s. The surface temperature data of the top layer were used to calculate the average and standard deviation values. Each test was repeated twice.

2.4. *Model applications*

2.4.1. *Simulation with three layers separated with polypropylene plastic sheets*

After validation, the simulation model was used to study the temperature distribution of chestnuts under different conditions. Since the highest temperatures appeared at contact points between top and middle layer at four corners of

Table 2 – Comparison of chestnut temperatures (°C) in three horizontal layers between simulation and experiment after 5.4 min RF heating at a fixed gap of 120 mm and initial temperature of 20 °C.

	Top layer			Middle layer			Bottom layer		
	Ave. temp.	Max. temp.	Min. temp.	Ave. temp.	Max. temp.	Min. temp.	Ave. temp.	Max. temp.	Min. temp.
Simulated	48.84 ± 3.65	90.74 ± 5.42	37.46 ± 3.31	52.74 ± 3.72	69.86 ± 4.86	29.38 ± 3.45	49.98 ± 3.31	65.41 ± 4.57	32.01 ± 3.16
Experimental	48.60 ± 2.71	100.25 ± 4.21	35.7 ± 2.47	52.70 ± 3.14	87.00 ± 3.94	42.25 ± 2.32	50.17 ± 2.48	80.20 ± 3.71	42.95 ± 2.62

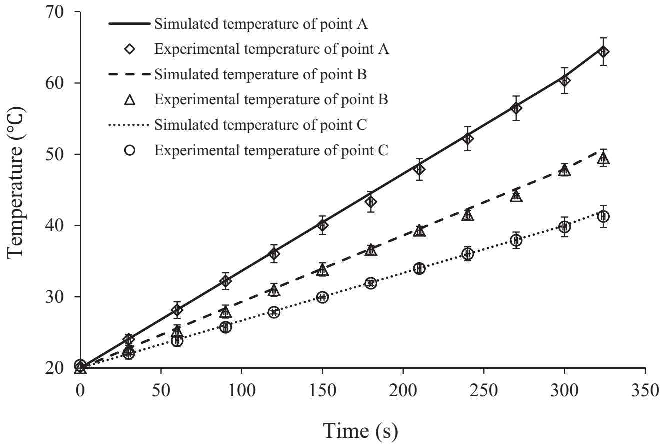

Fig. 4 – Validation of the computer simulation results by comparing experimental data with simulated temperature-time histories of chestnuts at locations A–C during RF heating.

the container, three layers were separated with two 0.2 cm thick polypropylene plastic sheets with an area of 18 × 24 cm^2 during RF heating. Then, simulated results (average temperature, highest temperature, and heating uniformity index) were compared with experimental ones.

2.4.2. *Simulation with single layer*

Since the highest temperature appeared at contact points between top and middle layer and the heating uniformity index was different from layer to layer, single layer chestnuts were placed into the plastic container and heated by RF energy. After simulation, the average temperature and heating uniformity index were validated by experiment.

2.4.3. *Simulation with mixing conditions*

On the one hand, the corners and edges heating were observed in mung beans (Huang et al., 2015b), wheat (Chen et al., 2015), wheat flour (Tiwari et al., 2011b), and chestnuts. On the other hand, the temperatures of contact points were higher than those in a single particle chestnut. So, mixing may be an effective method to eliminate the adverse effects from overheating at contact points of corners and edges in the container, and then improve heating uniformity of chestnuts. To simulate temperature distributions of chestnuts subjected to RF heating under mixing conditions, the following assumptions were considered. First, the temperature distributions of chestnuts were assumed to be uniform after each mixing (Wang et al., 2007b; Chen et al., 2015). Second, the mass and momentum transfers of moisture were neglected due to a short time RF heating.

During 5.4 min RF heating, two mixing processes were conducted with an interval of 1.8 min. In the simulation model, after one time mixing for one interval RF heating, the average temperature of chestnuts was regarded as the initial temperature for next interval RF heating until two mixing processes were completed. The temperature drop (ΔT, °C) due to heat loss during each mixing process was considered in simulation model as follows:

$$\Delta T = \frac{hA(T_{av} - T_{initial})\Delta t}{\rho C_p V} \quad (8)$$

where h is convective heat coefficient, which was estimated to be 28 W m^{-2} K^{-1} with forced convection during the whole mixing process (Wang et al., 2007b), A and V are the whole surface areas (0.1368 m^2) and volume (0.002592 m^3), respectively. T_{av} and $T_{initial}$ are the final average temperatures of the chestnuts after RF heating prior to each mixing and the ambient air temperature (20 °C), respectively. Δt is the total time (60 s) taken during each mixing process.

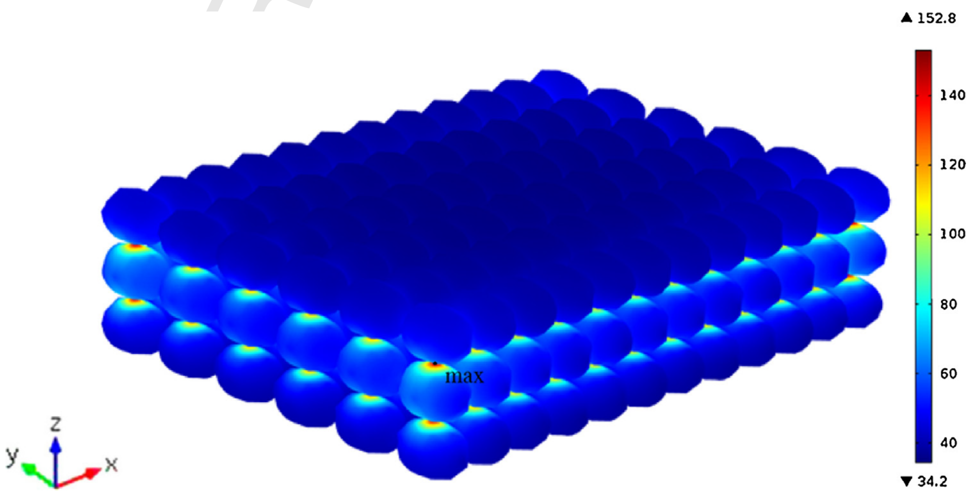

Fig. 5 – Simulated temperature distributions of chestnuts after 5.4 min RF heating with an electrode gap of 120 mm and initial temperature of 20 °C.

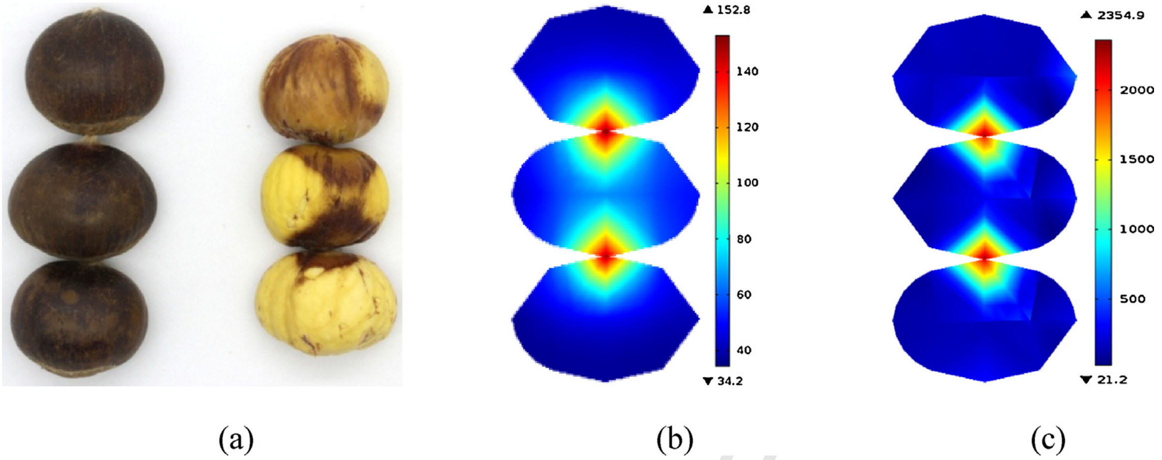

Fig. 6 – Comparison of experimental (a), simulated (b) temperature (°C), and E-field (c) (V/m) distribution of chestnuts at corners of container after 5.4 min RF heating with an electrode gap of 120 mm and initial temperature of 20 °C.

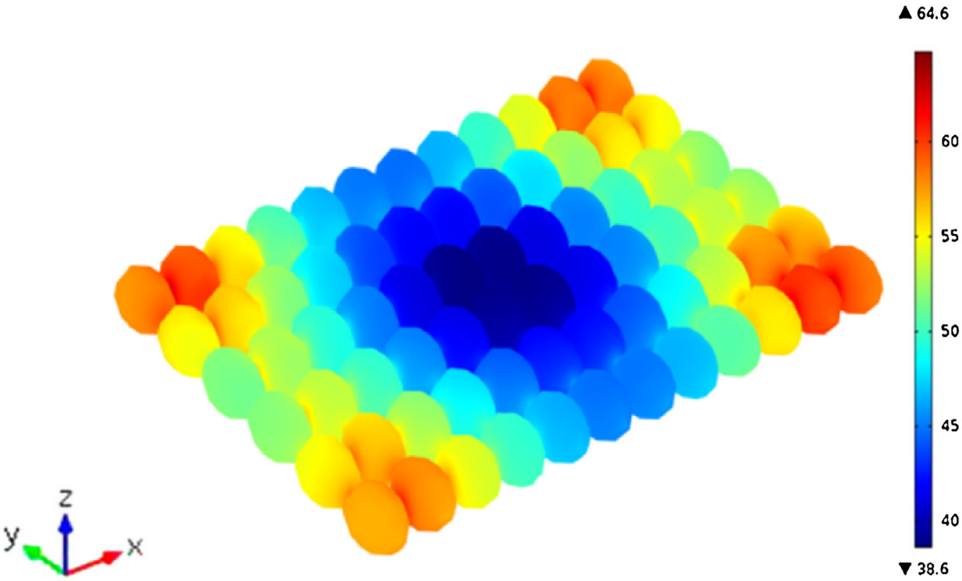

Fig. 7 – Simulated temperature distribution of single layer chestnuts after RF heating with an electrode gap of 120 mm and initial temperature of 20 °C.

3. Results and discussion

3.1. *Model development and validation*

Fig. 3 shows a comparison between simulated and experimental temperature distributions of chestnuts in three layers. Results demonstrated that the simulated and experimental temperature distribution patterns for all three layers were in good agreement. Corners and edges heating was obviously observed for all layers and cold spots were found at the center part in each layer. To obtain the internal temperature distribution of bulk chestnuts, the simulation was applied to the whole geometry of each individual chestnut in three layers. The simulation results showed that the temperature of a single chestnut was higher in its center except for those at corners of the container. But this phenomenon was not found in experimental temperature distribution since the experimental thermal images of RF treated chestnuts only indicated the surface temperature of the chestnuts. At corners of the container, the temperature of contact points was higher than other parts of chestnuts. Electrical field concentrated at corners and edges of the sample was caused by the electrical field refraction and reflection, resulting in higher temperature distributions on these parts. Values of the experimentally determined temperature and the simulated one matched well except for corners of the sample where the simulated average temperatures in the top and middle layers were slightly higher than those determined by experiments but opposite results were found in the bottom layer (Table 2). Generally, these small temperature differences between simulation and experiment could be ignored since these relative temperature differences were 0.5%, 0.0% and 0.4% in the top, middle and bottom layers, respectively. Temperature-time histories of chestnuts at the points A–C in the middle layer were also compared (Fig. 4). Simulated and experimental temperature-time histories of chestnuts at these points (A–C) were also in good agreement. A similar heating rate of 8.33, 5.56 and 4.07 °C min^{-1} for chestnuts at the points A–C, respectively, was obtained both in simulation and experiment during the heating period. Table 2 compares simulated and experimental average and standard deviation temperatures for chestnuts in three horizontal layers after 5.4 min RF heating. The experimental average temperatures matched well with the simulated ones, while the simulated temperatures in each layer were slightly lower than the experimental ones. This may be due to experimental temperature data obtained at the end of experiments while simulated temperatures were recorded during simulation. Both simulated and experimental results showed that the average temperature values were higher at middle layers followed by bottom and top layers. Similar results were found in soybean (Huang et al., 2015c), wheat (Chen et al., 2015), and wheat flour (Tiwari et al., 2011b).

This simulation method based on single particle approach was working well for large size samples, such as chestnuts and walnuts, as demonstrated in this study. It would be possible for applying this simulation approach to small particle samples, such as soybean and wheat as soon as the enough computer capacitance could be provided to obtain convergence results through the fine meshes. On the other hand, the simulation results based on single particle approach could be close to those in bulk samples obtained by mixing equations due to small voids in small particle samples.

3.2. *Validated temperature distribution in corners of the container*

Fig. 5 shows simulated temperature profiles of chestnuts after 5.4 min RF heating with an electrode gap of 120 mm. Highest temperature (152.84 °C) of treated chestnuts, was three times the average temperature (50.50 °C) of treated chestnuts, located in the contact points between top and middle layers at four corners. To understand the temperature profile of chestnuts at the corners, comparison of experimental and simulated temperature distributions of top, middle, and bottom layers at the corners of container is shown in Fig. 6(a, b). The temperatures of the contact points were higher than other parts of chestnuts both in experimental and simulated samples. This phenomenon may be caused by concentrated E-fields distributions around those contact areas. As shown in Fig. 6(c), the E-fields intensity of contact points was higher than other parts. While the RF power density at any location is proportional to the square of E-field, higher temperatures were observed at the corners of the container with higher E-field intensity. This over-heating phenomenon appeared at the contact points of sweet cherries when cherries treated with RF energy in air at the points of contact with container or with other fruits (Ikediala et al., 2002). Since chestnuts were a heat-sensitive nut and the chestnut skin was easy to be brown when the temperature was above 70 °C (Hou et al., 2015b). The color of chestnut skin became brown at both contact points and areas near the contact point in experiment, which matched well with simulated temperature distributions (Fig. 6).

3.3. *Heating uniformity improvement in chestnuts*

3.3.1. *Layers separated with plastic sheet*

Table 3 showed heating uniformity index of simulated and experimental results of chestnuts at three horizontal layers separated with or without two plastic sheets after 5.4 min RF heating. By adding plastic sheets, heating uniformity index of computer simulation model was reduced from 0.148 to 0.111, which was in good agreement with that of experiment. Heating uniformity was improved, which may be caused by less concentrated E-fields at the contact points separated with the plastic sheets, resulting in the reduced highest temperatures.

Table 3 – Comparison of chestnut temperatures (°C) and heating uniformity index (HUI) between simulation and experiment in three horizontal layers separated with or without two plastic sheets at a fixed electrode gap of 120 mm.

		Top layer			Middle layer			Bottom layer		
		Ave. temp.	Max. temp.	HUI	Ave. temp.	Max. temp.	HUI	Ave. temp.	Max. temp.	HUI
Simulated	With	54.41 ± 2.32	81.39 ± 3.76	0.051 ± 0.004	48.06 ± 2.14	59.82 ± 3.37	0.030 ± 0.002	48.67 ± 2.17	55.28 ± 3.19	0.041 ± 0.003
	Without	48.84 ± 3.65	90.74 ± 5.42	0.127 ± 0.007	52.74 ± 3.72	69.86 ± 4.86	0.135 ± 0.008	49.98 ± 3.31	65.41 ± 4.57	0.127 ± 0.007
Experimental	With	49.87 ± 1.51	76.97 ± 3.78	0.136 ± 0.008	52.14 ± 2.36	68.93 ± 3.14	0.126 ± 0.007	50.02 ± 1.74	61.72 ± 3.19	0.129 ± 0.007
	Without	48.60 ± 2.71	100.25 ± 4.21	0.219 ± 0.014	52.70 ± 3.14	87.00 ± 3.94	0.184 ± 0.011	50.17 ± 2.48	80.20 ± 3.71	0.188 ± 0.011

Table 4 – Comparison of chestnut temperatures (°C) and heating uniformity index (HUI) in three horizontal layers between simulation and experiment with mixing at a fixed gap of 120 mm.

	Top layer		Middle layer		Bottom layer	
	Ave. temp.	HUI	Ave. temp.	HUI	Ave. temp.	HUI
Simulation	48.70 ± 1.11	0.031 ± 0.012	52.53 ± 1.37	0.054 ± 0.013	49.73 ± 1.63	0.032 ± 0.012
Experiment	48.32 ± 1.72	0.077 ± 0.026	51.76 ± 1.68	0.071 ± 0.008	49.62 ± 2.22	0.061 ± 0.007

3.3.2. *Simulation with single layer*

Fig. 7 showed the temperature distribution of simulated chestnuts with single layer when the chestnuts were heated by RF energy with electrode gap of 12 cm. After RF heating, the average temperature, highest temperature, and heating uniformity index were 50.07 °C, 64.69 °C, and 0.0355, respectively. At the same time, the heating uniformity index was 0.0803 when the chestnuts were heated from 20 °C to 50.01 °C (average temperature) in experiment. Both the simulation and experiment results indicated that the heating uniformity index of single layer chestnuts was better than that of three layers. This may be caused by no contact points along the Z-axis.

3.3.3. *Simulation with mixing conditions*

Table 4 lists average temperature and heating uniformity index of chestnuts in three horizontal layers with two mixing processes during RF heating. The heating uniformity index in both simulation and experiment was reduced as compared without mixing (Table 3), which means mixing can improve heating uniformity of chestnuts. Position of chestnuts and contact points were randomly changed with mixing, resulting in better heating uniformity. After one-, two-, and three-time mixings, the heating uniformity index in wheat samples showed decreasing trend with the increasing mixing times, indicating that mixing can also improve heating uniformity (Chen et al., 2015).

4. Conclusions

A computer simulation model was developed for RF heating bulk chestnuts based on single particle approach in a 6 kW, 27.12 MHz RF unit. Results from computer simulation and experimental methods showed a good agreement for the temperature distribution in three horizontal layers of chestnuts packed in the plastic container. Simulated and experimental results both showed that highest temperatures were located at the sample contact points of the four corners in the container. The validated simulation model was further used to study the influence of layers separated with plastic sheets, single layer, and mixing conditions on the temperature distribution of RF heated chestnuts. Both simulated and experimental results showed that the better RF heating uniformity was achieved when the three layers of chestnuts were separated with two plastic sheets, heated with a single layer, and mixing during RF heating. The developed simulation model can help understand the temperature distributions in a single chestnut and improve the heating uniformity of bulk chestnuts when subjected to RF heating.

Acknowledgments

This research was conducted in the College of Mechanical and Electronic Engineering, Northwest A&F University, and supported by research grants from General Program of National Natural Science Foundation of China (No. 31371853) and Program of Introducing International Advanced Agricultural Science and Technologies (948 Program) of Ministry of Agriculture of China (2014-Z21).

References

Alfaifi, B., Tang, J., Jiao, Y., Wang, S., Rasco, B., Jiao, S., Sablani, S., 2014. Radio frequency disinfestation treatments for dried fruit: model development and validation. J. Food Eng. 120, 268–276.

Antonio, A.L., Fernandes, Â., Barreira, J.C.M., Bento, A., Botelho, M.L., Ferreira, I.C.F.R., 2011. Influence of gamma irradiation in the antioxidant potential of chestnuts (*Castanea sativa* Mill.) fruits and skins. Food Chem. Toxicol. 49 (9), 1918–1923.

Birla, S.L., Wang, S., Tang, J., 2008. Computer simulation of radio frequency heating of model fruit immersed in water. J. Food Eng. 84 (2), 270–280.

Carocho, M., Barreira, J.C.M., Antonio, A.L., Bento, A., Kaluska, I., Ferreira, I.C.F.R., 2012. Effects of electron-beam radiation on nutritional parameters of portuguese chestnuts (*Castanea sativa* Mill.). J. Agric. Food Chem. 60 (31), 7754–7760.

Chen, L., Wang, K., Li, W., Wang, S., 2015. A strategy to simulate radio frequency heating under mixing conditions. Comput. Electron. Agric. 118, 100–110.

Chenlo, F., Moreira, R., Chaguri, L., Torres, M.D., 2009. Note. sugar, moisture contents, and color of chestnuts during different storage regimes. Food Sci. Technol. Int. 15 (2), 169–178.

Choi, C.M.T., 1991. Finite element modeling of the RF heating process. Magn. IEEE Trans. 27 (5), 4227–4230.

COMSOL material library, COMSOL, Multiphysics, V4.3a, Burlington, MA, USA, 2012.

Dev, S.R.S., Kannan, S., Gariepy, Y., 2012. Optimization of radio frequency heating of in-shell eggs through finite element modeling and experimental trials. Prog. Electromagn. Res. 45 (2), 203–222.

Gao, H., Liu, S., Shi, P., 2011. Progress of Chinese chestnut process technology and production model. Food Sci. 32, 141–143.

Gao, M., Tang, J., Wang, Y., Powers, J., Wang, S., 2010. Almond quality as influenced by radio frequency heat treatments for disinfestation. Postharvest Biol. Technol. 58 (3), 225–231.

Guo, W., Wu, X., Zhu, X., Wang, S., 2011. Temperature-dependent dielectric properties of chestnut and chestnut weevil from 10 to 4500 MHz. Biosyst. Eng. 110 (3), 340–347.

Hansen, J.D., Hara, A.H., Tenbrink, V.L., 1992. Vapor heat: a potential treatment to disinfest tropical cut flowers and foliage. HortScience 27 (2), 139–143.

Hossan, M.R., Byun, D., Dutta, P., 2010. Analysis of microwave heating for cylindrical shaped objects. Int. J Heat Mass Transf. 53 (23–24), 5129–5138.

Hou, L., Hou, J., Li, Z., Johnson, J.A., Wang, S., 2015a. Validation of radio frequency treatments as alternative non-chemical methods for disinfesting chestnuts. J. Stored Prod. Res. 63C, 75–79.

Hou, L., Ling, B., Wang, S., 2014. Development of thermal treatment protocol for disinfesting chestnuts using radio frequency energy. Postharvest Biol. Technol. 98C, 65–71.

Hou, L., Ling, B., Wang, S., 2015b. Kinetics of color degradation of chestnut kernel during thermal treatment and storage. Int. J. Agric. Biol. Eng. 8 (4), 106–115.

Huang, Z., Chen, L., Wang, S., 2015a. Computer simulation of radio frequency selective heating of insects in soybeans. Int. J. Heat Mass Transf. 90, 406–417.

Huang, Z., Zhu, H., Wang, S., 2015b. Finite element modeling and analysis of radio frequency heating rate in mung beans. Trans. ASABE 58 (1), 149–160.
Huang, Z., Zhu, H., Yan, R., Wang, S., 2015c. Simulation and prediction of radio frequency heating in dry soybeans. Biosyst. Eng. 129, 34–47.
Ikediala, J.N., Hansen, J.D., Tang, J., Drake, S.R., Wang, S., 2002. Development of a saline water immersion technique with RF energy as a postharvest treatment against codling moth in cherries. Postharvest Biol. Technol. 24 (1), 25–37.
Jiao, S., Johnson, J.A., Tang, J., Mattinson, D.S., Fellman, J.K., Davenport, T.L., Wang, S., 2013. Tolerance of codling moth, and apple quality associated with lowpressure/low temperature treatments. Postharvest Biol. Technol. 85, 136–140.
Jiao, S., Johnson, J.A., Tang, J., Wang, S., 2012. Industrial-scale radio frequency treatments for insect control in lentils. J. Stored Prod. Res. 48, 143–148.
Jiao, Y., Shi, H., Tang, J., Li, F., Wang, Shaojin, 2015. Improvement of radio frequency (RF) heating uniformity on low moisture foods with polyetherimide (PEI) blocks. Food Res. Int. 74, 106–114.
Jiao, Y., Tang, J., Wang, S., 2014. A new strategy to improve heating uniformity of low moisture foods in radio frequency treatment for pathogen control. J. Food Eng. 141, 128–138.
Korel, F., Balaban, M.Ö., 2006. Composition, color and mechanical characteristics of pretreated candied chestnuts. Int. J. Food Prop. 9 (3), 559–572.
Moreira, R., Chenlo, F., Chaguri, L., Vázquez, G., 2011. Air drying and colour characteristics of chestnuts pre-submitted to osmotic dehydration with sodium chloride. Food Bioprod. Process. 89 (2), 109–115.
Moreira, R., Chenlo, F., Torres, M.D., Rama, B., 2013. Influence of the chestnuts drying temperature on the rheological properties of their doughs. Food Bioprod. 91 (1), 7–13.
Marshall, M., Metaxas, A., 1998. Modeling of the radio frequency electric field strength developed during the RF assisted heat pump drying of particulates. J. Microwave Power Electromagn. Energy 33 (3), 167–177.
Nelson, S.O., 1991. Dielectric properties of agricultural product measurements and applications. IEEE Trans. 26 (5), 845–869.
Pan, L., Jiao, S., Gautz, L., Tu, K., Wang, S., 2012. Coffee bean heating uniformity and quality as influenced by radio frequency treatments for postharvest disinfestations. Trans. ASABE 55 (6), 2293–2300.
Romano, V., Marra, F., 2008. A numerical analysis of radio frequency heating of regular shaped foodstuff. J. Food Eng. 84 (3), 449–457.
Sahin, S., Sumnu, S.G., 2006. Physical Properties of Food. Springer, New York.
Tiwari, G., Wang, S., Tang, J., Birla, S.L., 2011a. Analysis of radio frequency (RF) power distribution in dry food materials. J. Food Eng. 104 (4), 548–556.
Tiwari, G., Wang, S., Tang, J., Birla, S.L., 2011b. Computer simulation model development and validation for radio frequency (RF) heating of dry food materials. J. Food Eng. 105 (1), 48–55.
Uyar, R., Bedane, T.F., Erdogdu, F., Palazoglu, T.K., Farag, K.W., Marra, F., 2015. Radio-frequency thawing of food products—a computational study. J. Food Eng. 146, 163–171.
Uyar, R., Erdogdu, F., Sarghini, F., Marra, F., 2016. Computer simulation of radio-frequency heating applied to block-shaped foods: analysis on the role of geometrical parameters. Food Bioprod. Process. 98, 310–319.
Vasconcelos, M.C.D., Bennett, R.N., Rosa, E.A., Ferreira-Cardoso, J.V., 2010. Composition of european chestnut (*Castanea sativa* Mill.) and association with health effects: fresh and processed products. J. Sci. Food Agric. 90 (10), 1578–1589.
von Hippel, A.R., 1995. Dielectric Materials and Applications. Arctech House, Boston, USA.
Wang, S., Monzon, M., Johnson, J.A., Mitcham, E.J., Tang, J., 2007a. Industrial-scale radio frequency treatments for insect control in walnuts I: heating uniformity and energy efficiency. Postharvest Biol. Technol. 45 (2), 240–246.
Wang, S., Monzon, M., Johnson, J.A., Mitcham, E.J., Tang, J., 2007b. Industrial-scale radio frequency treatments for insect control in walnuts II: insect mortality and product quality. Postharvest Biol. Technol. 45 (2), 247–253.
Wang, S., Tang, J., Cavalieri, R.P., 2001. Modeling fruit internal heating rates for hot air and hot water treatments. Postharvest Biol. Technol. 22 (3), 257–270.

Please cite this article in press as: Hou, L., et al., Computer simulation model development and validation of radio frequency heating for bulk chestnuts based on single particle approach. Food Bioprod Process (2016), http://dx.doi.org/10.1016/j.fbp.2016.08.008